Development of a Semi-Analytic Nodal Method with Edge Segmentation for Two-Dimensional Triangular Geometry



2026년도 추계 한국원자력학회

Gyeongju Hwabaek International Convention Center(HICO),
Korea, October 28-30, 2026

Junwoo Lee [a], Yonghee Kim [a]

[a] Korea Advanced Institute of Science and Technology (KAIST)

Contents

1. **Introduction**
   - Objectives & Motivation
   - SENTRI

2. **Methodology**
   - Node definition & governing equation
   - Edge-segmented partial current
   - Basis functions
   - Source expansion
   - Solution Algorithm

3. **Numerical Results**
   - VVER440
   - VVER1000
   - MHTGR-350

4. **Conclusions & Future Works**

5. **References**

Contents

1. **Introduction**
   - Motivation & Objectives
   - SENTRI

2. **Methodology**
   - Node definition & governing equation
   - Edge-segmented partial current
   - Basis functions
   - Source expansion
   - Solution Algorithm

3. **Numerical Results**
   - VVER440
   - VVER1000
   - MHTGR-350

4. **Conclusions & Future Works**

5. **References**

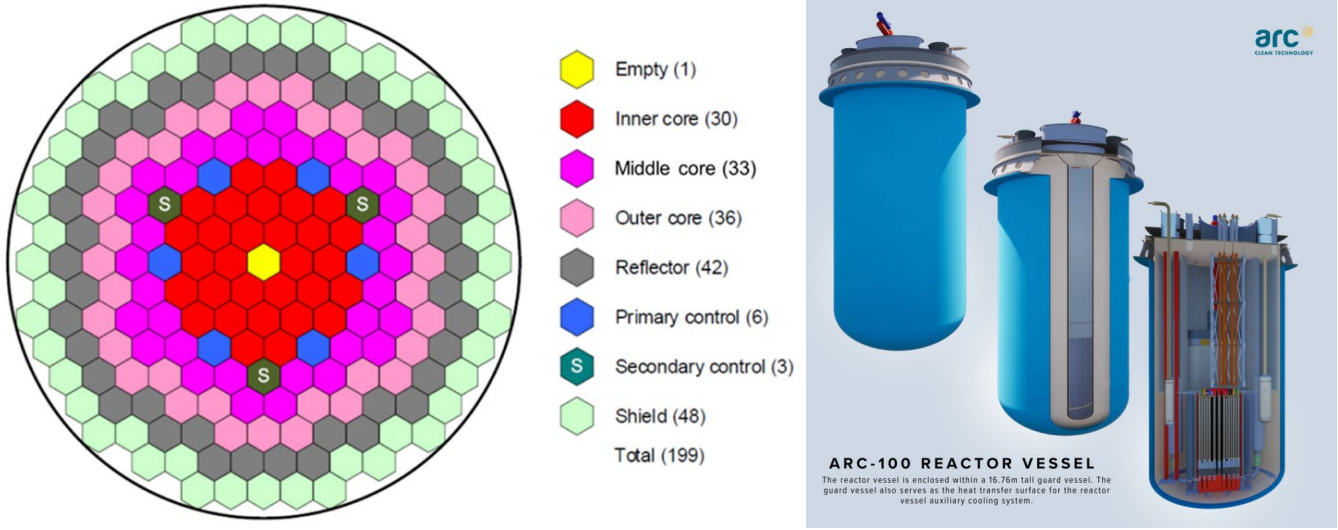
1. Introduction

❑ Background

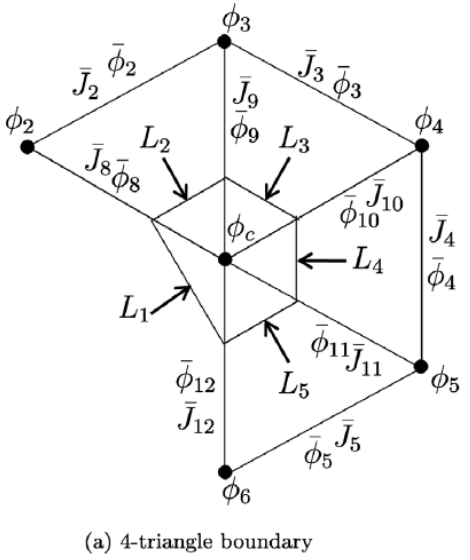
- Growing interest in hexagonal-lattice core for SMR designs [1]
- Development of numerous nodal codes based on hexagonal geometry

❑ Motivations (1/2)

- Triangular nodes: finer resolution and intra-hexagonal heterogeneity [9]
- No rigorous corner-point balance at the core boundary [9]
- Difficulty of using rigorous corner discontinuity factors (CDFs) in practical two-step analysis [15]



<Fig 1. ARC-100 Core Configuration[1]>



(a) 4-triangle boundary

<Fig 2. Corner-point flux at boundary>

1. Introduction

❑ Motivations (2/2)

- Corner-point flux as the coupling constraint in most methods
- Moments as the alternative, requiring DFs consistently defined for the moment [16]
- Practical use of DFs requires coupling mainly through surface-segment averages.

Table I. Comparison of nodal method for hexagonal-lattice cores

Method	Node	Flux representation	Internodal coupling	Source term
HOPEN[2]	Hexagon	Cubic polynomials	corner-point flux, surface flux	Cubic polynomials
AFEN[3,4]	Hexagon	Analytic functions	surface flux, moments	Analytic functions
ANC-H[6,7]	Hexagon	1D hyperbolic & polynomials	surface net currents	Quadratic polynomials
TPEN[8]	Triangle	Cubic polynomials	corner-point flux ,surface fluxes, moments	Cubic polynomials
TRIPEN[9]	Triangle	Cubic polynomials	corner-point flux, partial currents	Cubic polynomials
A-SANM[10]	Triangle	hyperbolic & polynomials	surface flux, corner-point flux, moments	Quadratic polynomials
ABFEM-T[11]	Arbitrary triangle	Analytic basis	partial current moments	Analytic basis
EFEN[12]	Arbitrary triangle	Exponential functions	Segmented partial current	Flat

1. Introduction

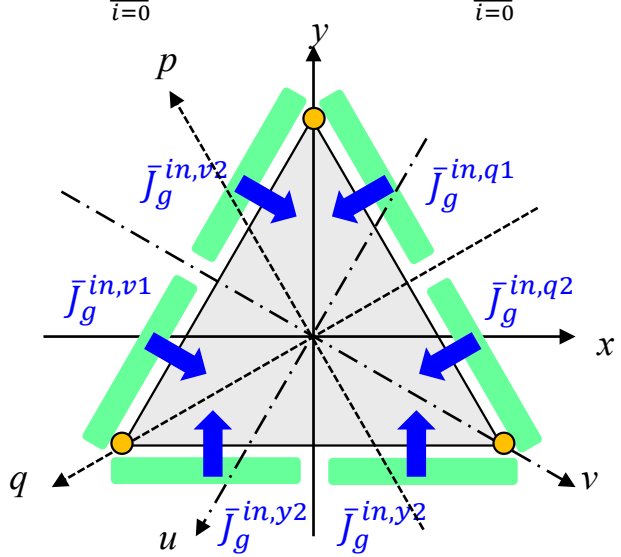
❑ Objectives

- Replace the corner-point flux with half-edge segmented partial currents [12]
- Extend the source approximation from a flat to a cubic polynomial expansion
- Capture steep intranodal flux gradients with a SANM-based hyperbolic & polynomial basis

SENTRI: **S**emi-analytic **E**dge segmentation **N**odal method for **TRI**angular geometry

➢ Half-edge segmented partial currents & SANM

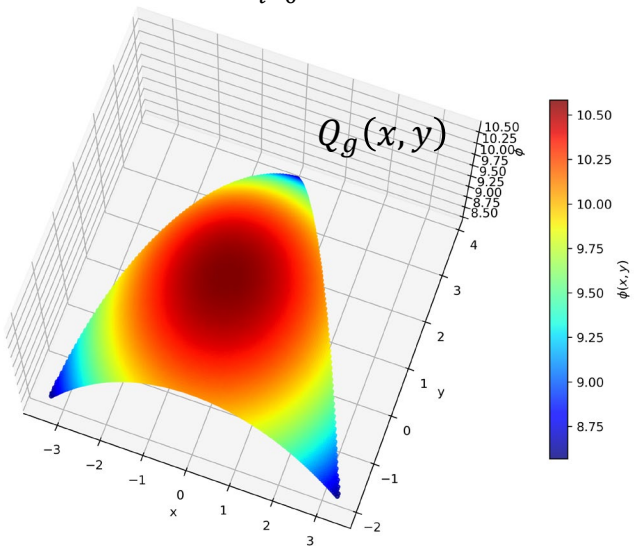
$$\phi_g(x,y) \coloneqq \sum_{i=0}^{5} a_{g,i} e^{\kappa_g (x\cos\theta_i + y\sin\theta_i)} + \sum_{i=0}^{8} c_{g,i}\varphi_i(x,y)\,.$$



<Fig 3. Half-edge segmented partial currents>

➢ Cubic polynomial source expansion

$$Q_g(x,y) \coloneqq \sum_{i=0}^{8} q_{g,i}\varphi_i(x,y)\,.$$



<Fig 4. Source term expansion>

Contents

1. Introduction
   - Motivation & Objectives
   - SENTRI

2. **Methodology**
   - Node definition & governing equation
   - Edge-segmented partial current
   - Basis functions
   - Source expansion
   - Solution Algorithm

3. Numerical Results
   - VVER440
   - VVER1000
   - MHTGR-350

4. Conclusions & Future Works

5. References

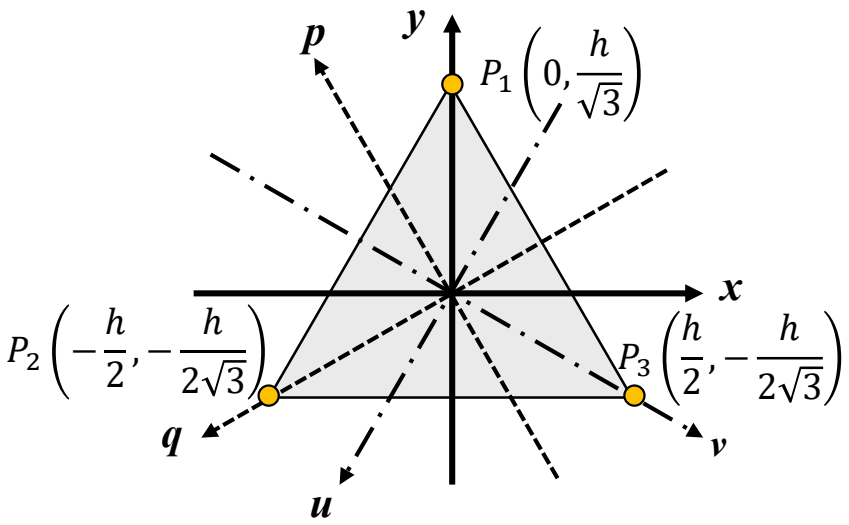
2. Methodology

❑ Node Definition

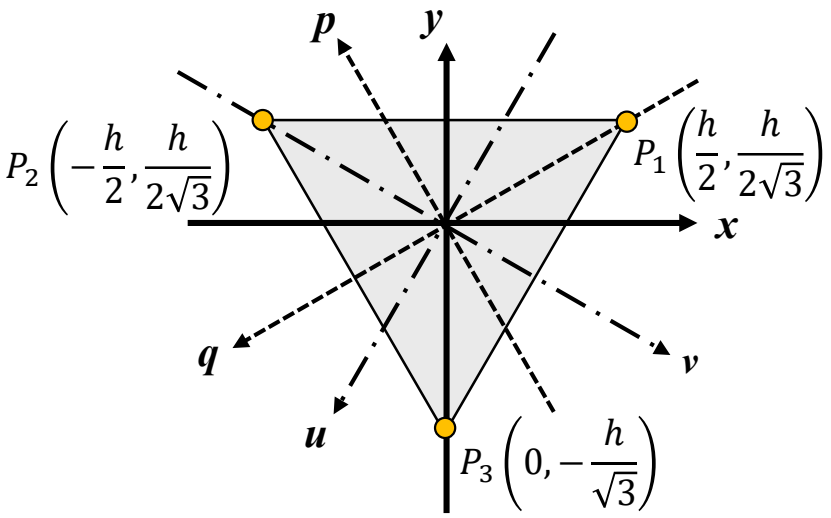
- A triangle-based nodal code for hexagonal core analysis
- Two types of equilateral triangles with side length h, upward and downward
- Rotated coordinates p, q, u, and v

$$p(x,y) = -\frac{1}{2}x + \frac{\sqrt{3}}{2}y, \qquad q(x,y) = -\frac{\sqrt{3}}{2}x - \frac{1}{2}y$$

$$u(x,y) = -\frac{1}{2}x - \frac{\sqrt{3}}{2}y, \qquad v(x,y) = \frac{\sqrt{3}}{2}x - \frac{1}{2}y$$



Upward node



Downward node

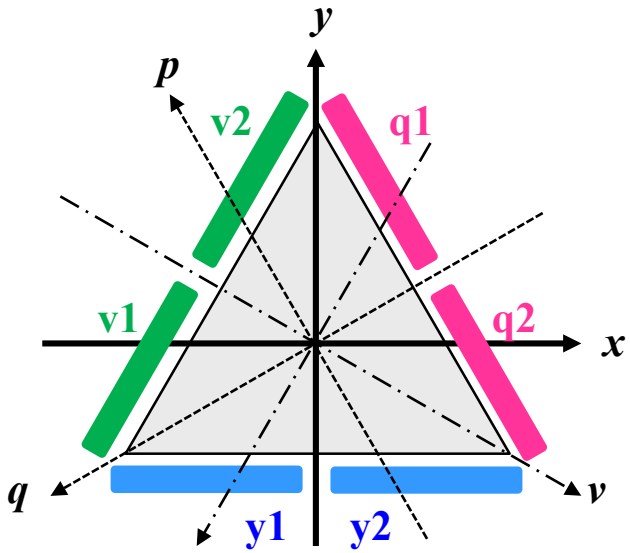
2. Methodology

❑ Edge-Segmented Partial Current

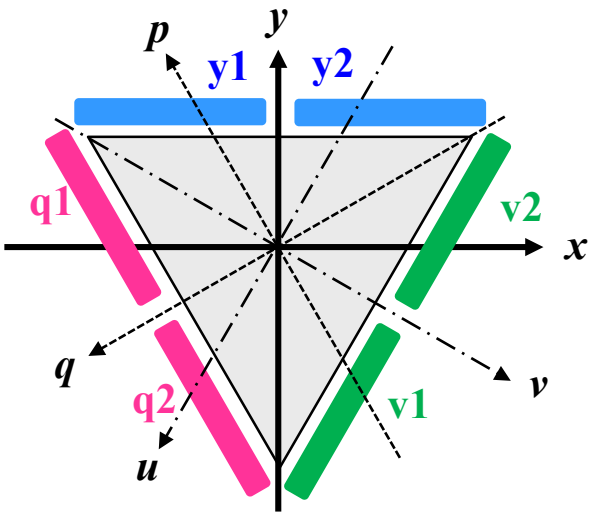
- Half-edge segments v1, v2, q1, q2, y1 and y2 defined
- Partial currents based on the P_1 approximation, with the outward direction from the node taken as positive
- Six incoming half-edge partial currents used as interface constraints replacing the corner-point flux

$$\bar{J}^{in}_{g,y1} \coloneqq \frac{2}{h}\int_{-h/2}^{0} dx \left[\frac{df_{g,y1}}{4}\phi_g(x,y) + \frac{D_g}{2}\nabla_{-y}\phi_g(x,y)\right].$$

$$\bar{J}^{out}_{g,y1} \coloneqq \frac{2}{h}\int_{-h/2}^{0} dx \left[\frac{df_{g,y1}}{4}\phi_g(x,y) - \frac{D_g}{2}\nabla_{-y}\phi_g(x,y)\right].$$



Upward node



Downward node

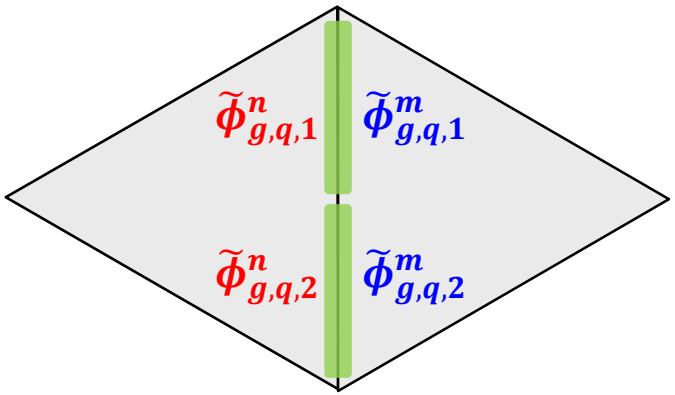
❑ Application of Discontinuity Factors (DFs) in SENTRI

- DFs are applied to each segmented edge or can also be applied to an entire edge
- 6 (segment-wise) or 3 (edge-wise) DFs per group per node are required
- Defined on surface averages, unlike point-wise CDFs that are arbitrary and approximated in practice [15]

$$\tilde{\phi}_{g,y1} \coloneqq \frac{2}{h}\int_{-h/2}^{0} dx\, \phi_g(x,y).$$

$$df_{g,k,i}^{n}\tilde{\phi}_{g,k,i}^{n} = df_{g,k,i}^{m}\tilde{\phi}_{g,k,i}^{m}, \qquad k \in \{v,q,y\}\ and\ i \in \{1,2\}.$$

➢ Half-edge segmented surface flux



➢ Surface flux & partial current continuity with DFs

$$df_{g,q,1}^{n}\tilde{\phi}_{g,q,1}^{n} = df_{g,q,1}^{m}\tilde{\phi}_{g,q,1}^{m}$$

$$df_{g,q,2}^{n}\tilde{\phi}_{g,q,2}^{n} = df_{g,q,2}^{m}\tilde{\phi}_{g,q,2}^{m}$$

$$\frac{1}{4}df_{g,q,1}^{n}\tilde{\phi}_{g,q,1}^{n} \pm \frac{1}{2}\bar{J}_{g,q,1}^{n} = \frac{1}{4}df_{g,q,1}^{m}\tilde{\phi}_{g,q,1}^{m} \mp \frac{1}{2}\bar{J}_{g,q,1}^{m}$$

$$\frac{1}{4}df_{g,q,2}^{n}\tilde{\phi}_{g,q,2}^{n} \pm \frac{1}{2}\bar{J}_{g,q,2}^{n} = \frac{1}{4}df_{g,q,2}^{m}\tilde{\phi}_{g,q,2}^{m} \mp \frac{1}{2}\bar{J}_{g,q,2}^{m}$$

$df_{g,q}^{n}$ can be used instead of $df_{g,q,1}^{n}$ and $df_{g,q,2}^{n}$

2. Methodology

❑ Basis Function

- Solving the 2-D multigroup neutron diffusion equation based on the SANM
- Expanding the source term into a cubic polynomial
- Intranodal flux as hyperbolic homogeneous plus polynomial particular solutions

$$\nabla^2\phi_g(x,y) - \kappa_g^2\phi_g(x,y) = -\frac{1}{D_g}Q_g(x,y), \qquad \kappa_g^2 \coloneqq \frac{\Sigma_{r,g}}{D_g}.$$

$$Q_g(x,y) \coloneqq \sum_{i=0}^{8} q_{g,i}\varphi_i(x,y) \cong \sum_{g'=1}^{G}\left[(1-\delta_{g,g'})\Sigma_{s,g'\to g} + \frac{\chi_g}{k_{eff}}\nu\Sigma_{f,g'}\right]\phi_{g'}(x,y) + L_g^Z(x,y).$$

$$\therefore \phi_g(x,y) \coloneqq \phi_g^H(x,y) + \phi_g^P(x,y).$$

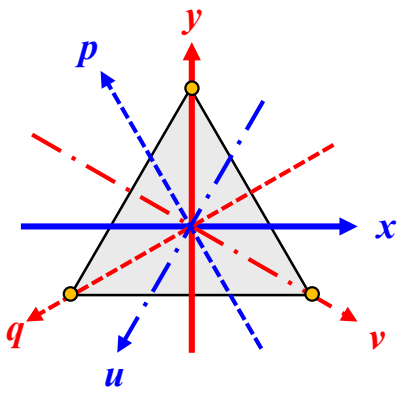
$$\nabla^2\phi_g^H(x,y) - \kappa_g^2\phi_g^H(x,y) = 0, \qquad \phi_g^H(x,y) = \sum_{i=0}^{5} a_{g,i}e^{\kappa_g(x\cos\theta_i + y\sin\theta_i)}.$$

$$\nabla^2\phi_g^P(x,y) - \kappa_g^2\phi_g^P(x,y) = -\frac{1}{D_g}\sum_{i=0}^{8} q_{g,i}\varphi_i(x,y), \qquad \phi_g^P(x,y) \coloneqq \sum_{i=0}^{8} c_{g,i}\varphi_i(x,y).$$

2. Methodology

❑ Basis Function

- Conventional bases (TPEN, TriPEN) defined along the edge-normal direction (*v*, *q*, and *y* in SENTRI)
  - ➢ Equal contributions to the partial currents on both of its half-edges
- Six $\bar{J}_g^{in}$ determine the six homogeneous-solution coefficients $a_{g,i}$ through a 6×6 linear system
- Singular 6 × 6 system $\bar{\bar{C}}$ with edge-normal bases → Rank 5
- Edge-tangential bases (*x*, *u*, and *p*) required to distinguish the two half-edges



<Fig 4. 6 directions in SENTRI>

$$\bar{\bar{C}} \quad \bar{a} \quad \bar{s}$$

$$\begin{pmatrix} C_{00} & C_{01} & \cdots & & \\ C_{10} & & & & \\ \vdots & & \ddots & & \vdots \\ & & & & C_{45} \\ & & \cdots & C_{54} & C_{55} \end{pmatrix} \begin{pmatrix} a_{g,0} \\ \vdots \\ a_{g,5} \end{pmatrix} = \begin{pmatrix} \bar{J}_{g,v1}^{in} - \bar{J}_{g,v1}^{in,P} \\ \vdots \\ \bar{J}_{g,y2}^{in} - \bar{J}_{g,y2}^{in,P} \end{pmatrix}$$

$$* \bar{J}_g^{in} = \bar{J}_g^{in,H} + \bar{J}_g^{in,P}$$

Edge-normal bases → $\mathrm{Rank}(\bar{\bar{C}}) = 5$

Edge-tangential bases → $\mathrm{Rank}(\bar{\bar{C}}) = 6$

$$\therefore \phi_g^H(x,y) = \sum_{i=0}^{5} a_{g,i} e^{\kappa_g (x\cos\theta_i + y\sin\theta_i)}, \qquad \theta_i = \frac{i\pi}{3}$$

2. Methodology

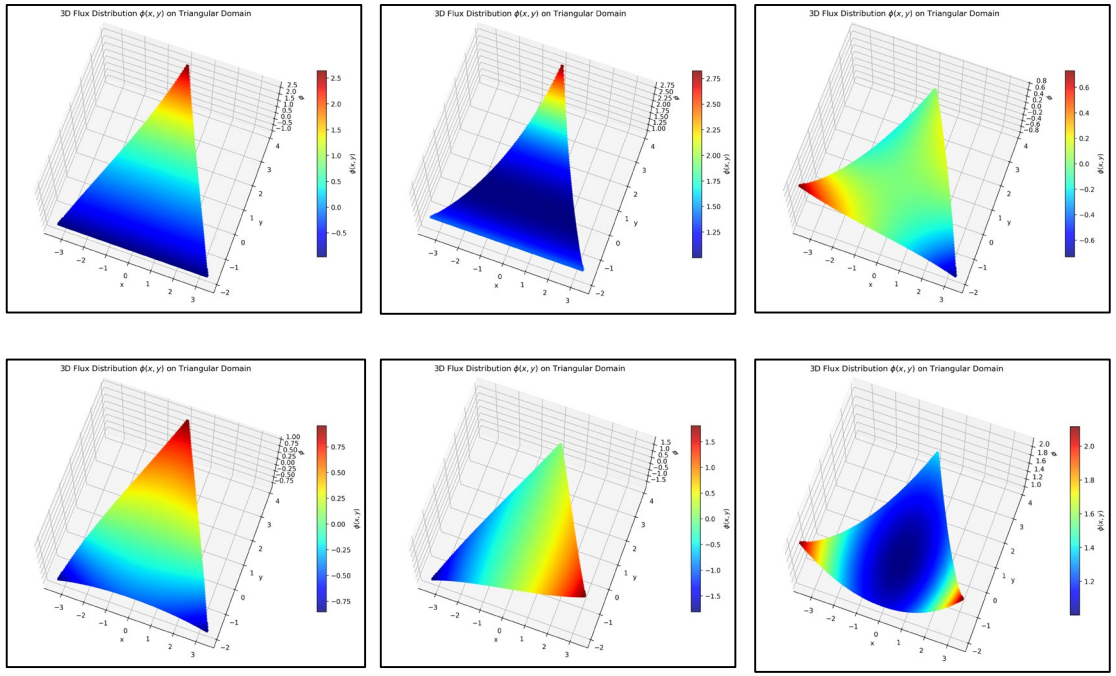
❑ Basis Function

- Conventional bases defined along the edge-normal direction (v, q, and y in SENTRI node)
- Singular 6×6 system $\overline{\overline{\boldsymbol{C}}}$ with edge-normal bases → Rank 5

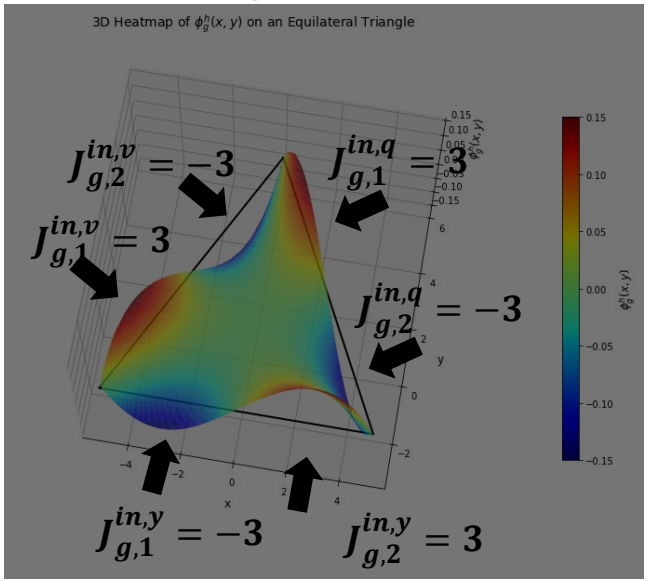
➢ Hyperbolic bases (edge-normal direction)

$$\phi_g^H(x,y) = \sum_{i=0}^{5} a_{g,i} e^{\kappa_g (x\cos\theta_i + y\sin\theta_i)}, \qquad \theta_i = \frac{\pi}{6} + \frac{i\pi}{3}$$

➢ 6 hyperbolic bases



➢ Target $\phi_g^H(x,y)$



No unique solution for $\overline{\boldsymbol{a}}$

2. Methodology

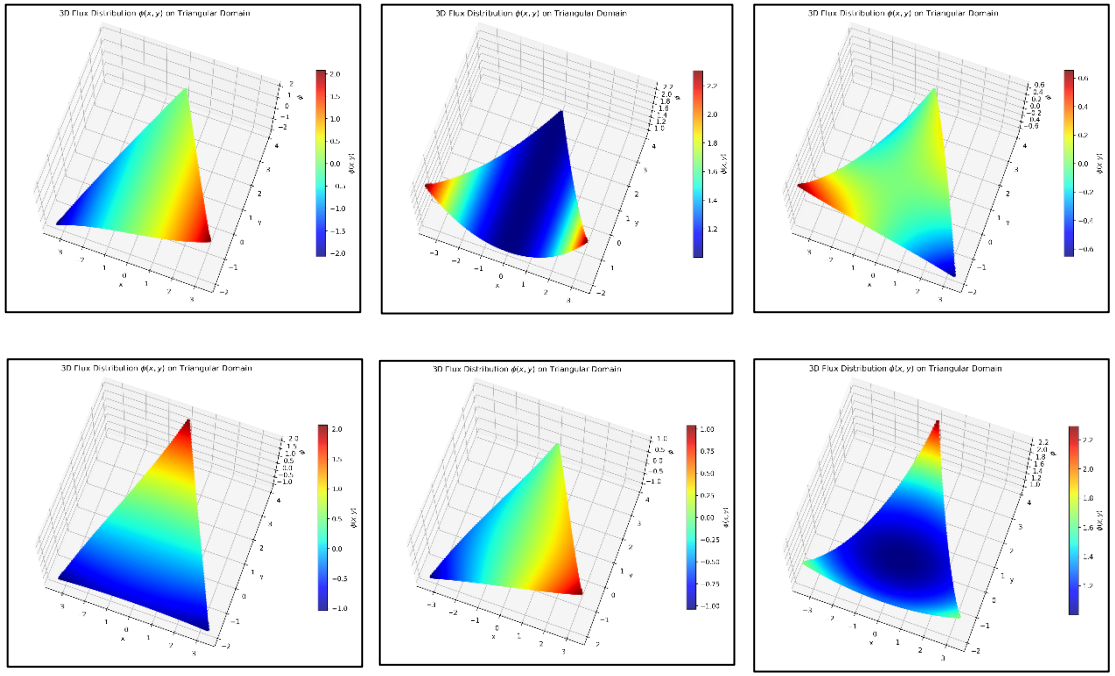
❑ Basis Function

- Building 6×6 system $\overline{\overline{C}}$ with edge-tangential bases → Rank 6
- Unique $a_{g,i}$ determined for any given partial currents

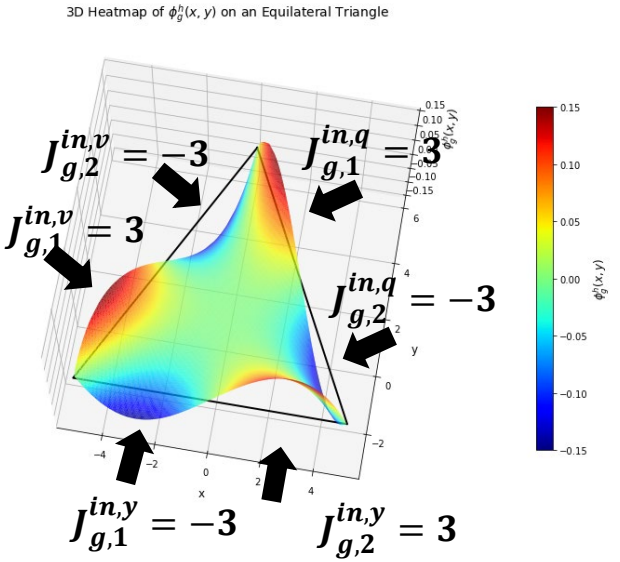
➢ Hyperbolic bases (edge-tangential direction)

$$\phi_g^H(x,y) = \sum_{i=0}^{5} a_{g,i} e^{\kappa_g (x\cos\theta_i + y\sin\theta_i)}, \qquad \theta_i = \frac{i\pi}{3}$$

➢ 6 hyperbolic bases



➢ Target $\phi_g^H(x,y)$



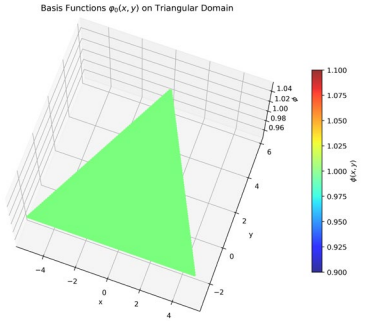
Unique solution for $\bar{a}$

2. Methodology

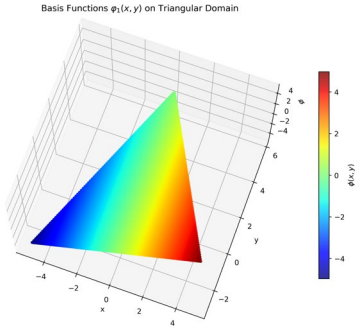
❑ Basis Function

- A total of 9 polynomial bases up to third order
- Higher-order terms constructed $(x^2, u^2, p^2, x^3, u^3, p^3)$ along the edge-tangential directions

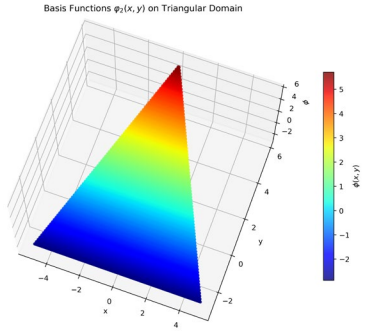
$\varphi_0 = 1$



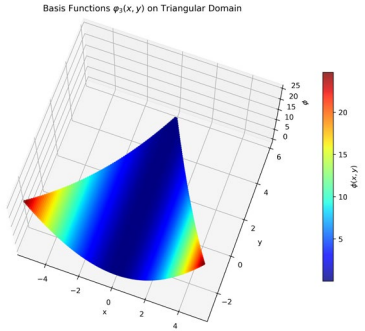
$\varphi_1 = x$



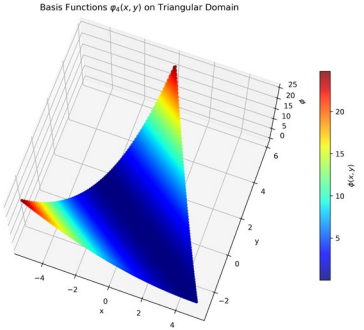
$\varphi_2 = y$



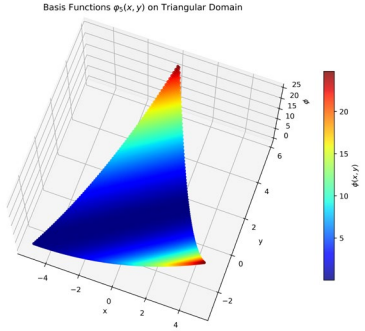
$\varphi_3 = x^2$



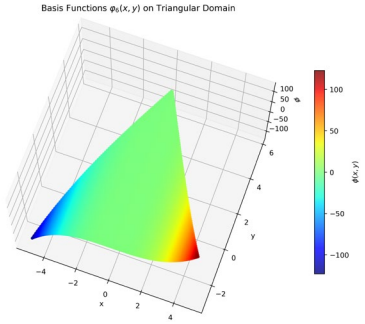
$\varphi_4 = u^2$



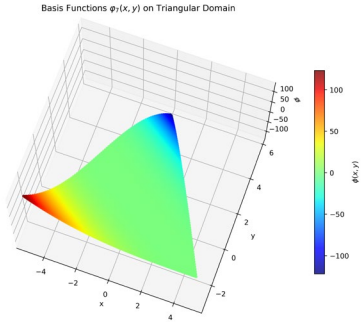
$\varphi_5 = p^2$



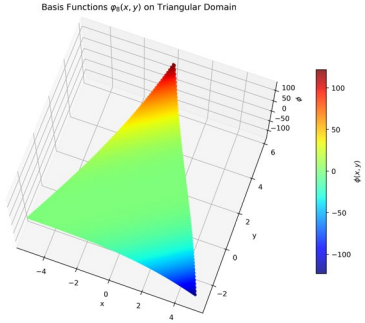
$\varphi_6 = x^3$



$\varphi_7 = u^3$



$\varphi_8 = p^3$



2. Methodology

❑ Source Expansion

- Source term is approximated by a cubic polynomial within the SANM framework
- General solution $\phi_g(x,y)$ recast into a polynomial form $\hat{\phi}_g(x,y)$
- **6** half-edge surface averaged fluxes preserves, with the remaining **3** coefficients determined by the WRM

➢ Source term

$$Q_g(x,y) = \sum_{g'=1}^{G}\left[(1-\delta_{g,g'})\Sigma_{s,g'\to g} + \frac{\chi_g}{k_{eff}}\nu\Sigma_{f,g'}\right]\phi_{g'}(x,y) + L_g^Z(x,y).$$

➢ Recasting $\phi_g(x,y)$ into $\hat{\phi}_g(x,y)$ (n = 0,1,2)

$$\iint_\Omega d\Omega\,\varphi_n(x,y)\left[\phi_g^H(x,y) + \phi_g^P(x,y) - \hat{\phi}_g(x,y)\right] = 0, \qquad where, \qquad \hat{\phi}_g(x,y) \coloneqq \sum_{i=0}^{8} b_{g,i}\varphi_i(x,y)\,.$$

➢ Source expansion

$$Q_g(x,y) \cong \sum_{g'=1}^{G}\left[(1-\delta_{g,g'})\Sigma_{s,g'\to g} + \frac{\chi_g}{k_{eff}}\nu\Sigma_{f,g'}\right]\sum_{i=0}^{8} b_{g',i}\varphi_i(x,y) + \sum_{i=0}^{2} L_{g,i}^Z\varphi_i(x,y)\,.$$

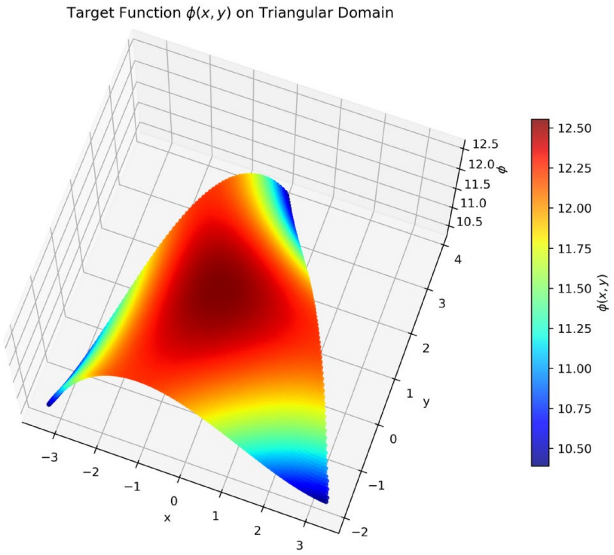
$$Q_g(x,y) = \sum_{i=0}^{8} q_{g,i}\varphi_i(x,y)\,.$$

2. Methodology

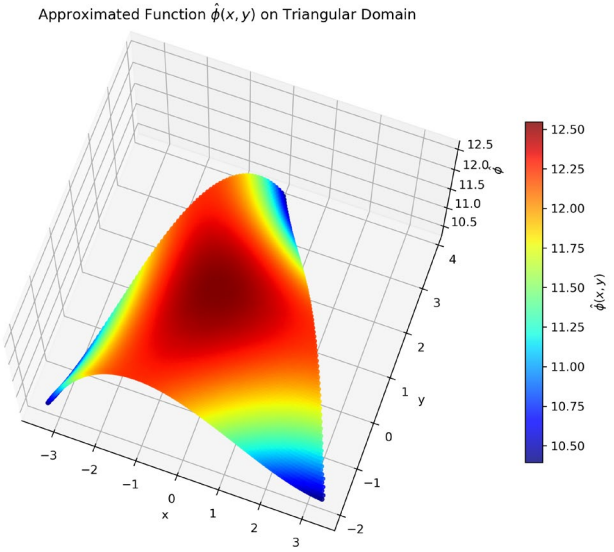
❑ Source Expansion

- Source term is approximated by a cubic polynomial within the SANM framework
- General solution $\phi_g(x,y)$ recast into a polynomial form $\hat{\phi}_g(x,y)$
- **6** half-edge surface averaged fluxes preserves, with the remaining **3** coefficients determined by the WRM

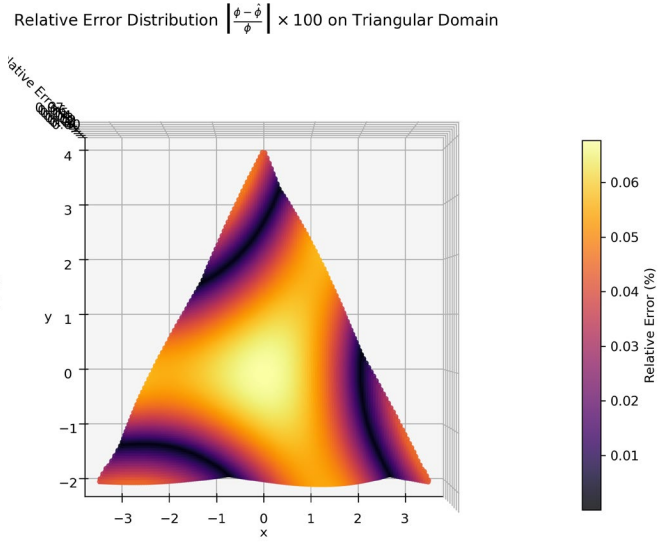
➢ $\phi_g(x,y)$



➢ $\hat{\phi}_g(x,y)$



➢ $\left|(\phi_g - \hat{\phi}_g)/\phi_g\right|$



RMS ≤ 0.1 %

2. Methodology

❑ Solution Algorithm

1. Source iteration for each group g

- Knowns: 6 incoming partial currents $\bar{J}_g^{in}$, node-averaged fixed source $\bar{Q}_g$, k_{eff}

① Guess the source term coefficients $q_{g,i}$
② Update the particular solution coefficients $c_{g,i}$ with $q_{g,i}$ and update $\bar{J}_g^{in,P}$
③ Update the homogeneous solution coefficients $a_{g,i}$ with $\bar{J}_g^{in} - \bar{J}_g^{in,P}$
④ Update the approximated solution coefficients $b_{g,i}$ with $a_{g,i}$, $c_{g,i}$
⑤ Update the source term coefficients $q_{g,i}$ with $b_{g,i}$, scaled to match $\bar{Q}_g$
⑥ Compare $q_{g,i}$ with the previous $q_{g,i}$. If converged, update $\bar{J}_g^{out}$. Otherwise, go to step 2.

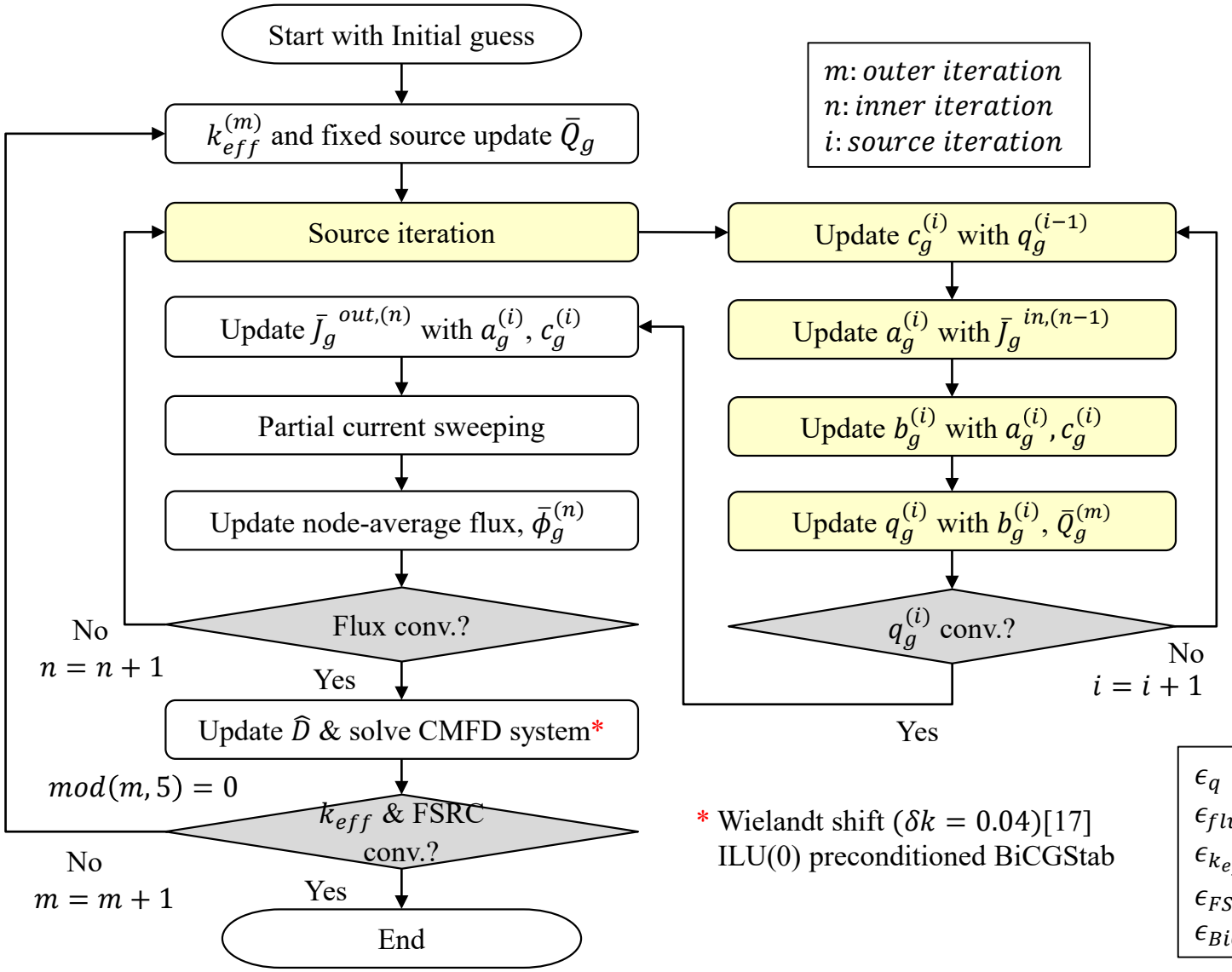
2. Inner iteration

① Partial current sweeping
② Update the node-average flux based on the nodal balance
③ Compare $\bar{\phi}_g$with the previous $\bar{\phi}_g$. If converged, update $\bar{J}_g$. Other wise, go to source iteration

3. Outer iteration

① Update the CMFD correction factor $\widehat{D}$ and the CMFD linear system
② Solve the CMFD linear system and compare the fission source and k_{eff}
③ If converged, end the calculation. Other wise, update $\bar{Q}_g$, k_{eff} and go to source iteration

❑ Solution Algorithm



* Wielandt shift ($\delta k = 0.04$)[17]
ILU(0) preconditioned BiCGStab

$\epsilon_q = 1.0 \times 10^{-4}$
$\epsilon_{flux} = 1.0 \times 10^{-6}$
$\epsilon_{k_{eff}} = 1.0 \times 10^{-7}$
$\epsilon_{FSRC} = 1.0 \times 10^{-5}$
$\epsilon_{BiCG} = 1.0 \times 10^{-9}$

Contents

1. Introduction
   - Motivation & Objectives
   - SENTRI

2. Methodology
   - Node definition & governing equation
   - Edge-segmented partial current
   - Basis functions
   - Source expansion
   - Solution Algorithm

3. **Numerical Results**
   - VVER440
   - VVER1000
   - MHTGR-350

4. Conclusions & Future Works

5. References

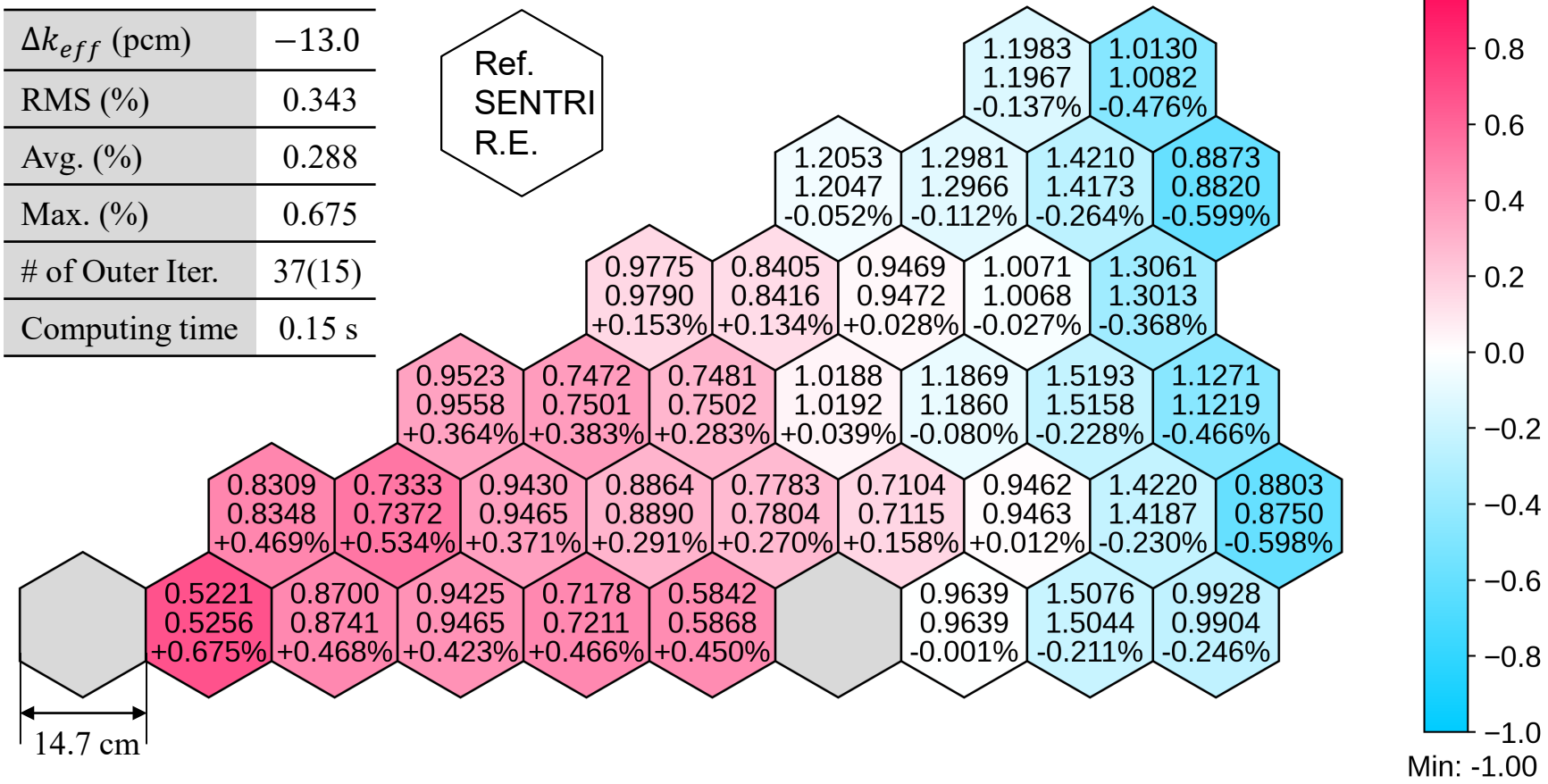
3. Numerical Results

❑ **VVER-440 2D 2G** ($\alpha = 0.500$)

- $k_{eff} = 1.009570$ ($\Delta k_{eff} = -13.0\ pcm$)
- RMS = 0.343 % | Avg. Abs. Rel. Err. = 0.288 % | Max. Abs. Rel. Err. = 0.675 %

VVER-440 2D (α=0.5) Power Relative Error Distribution

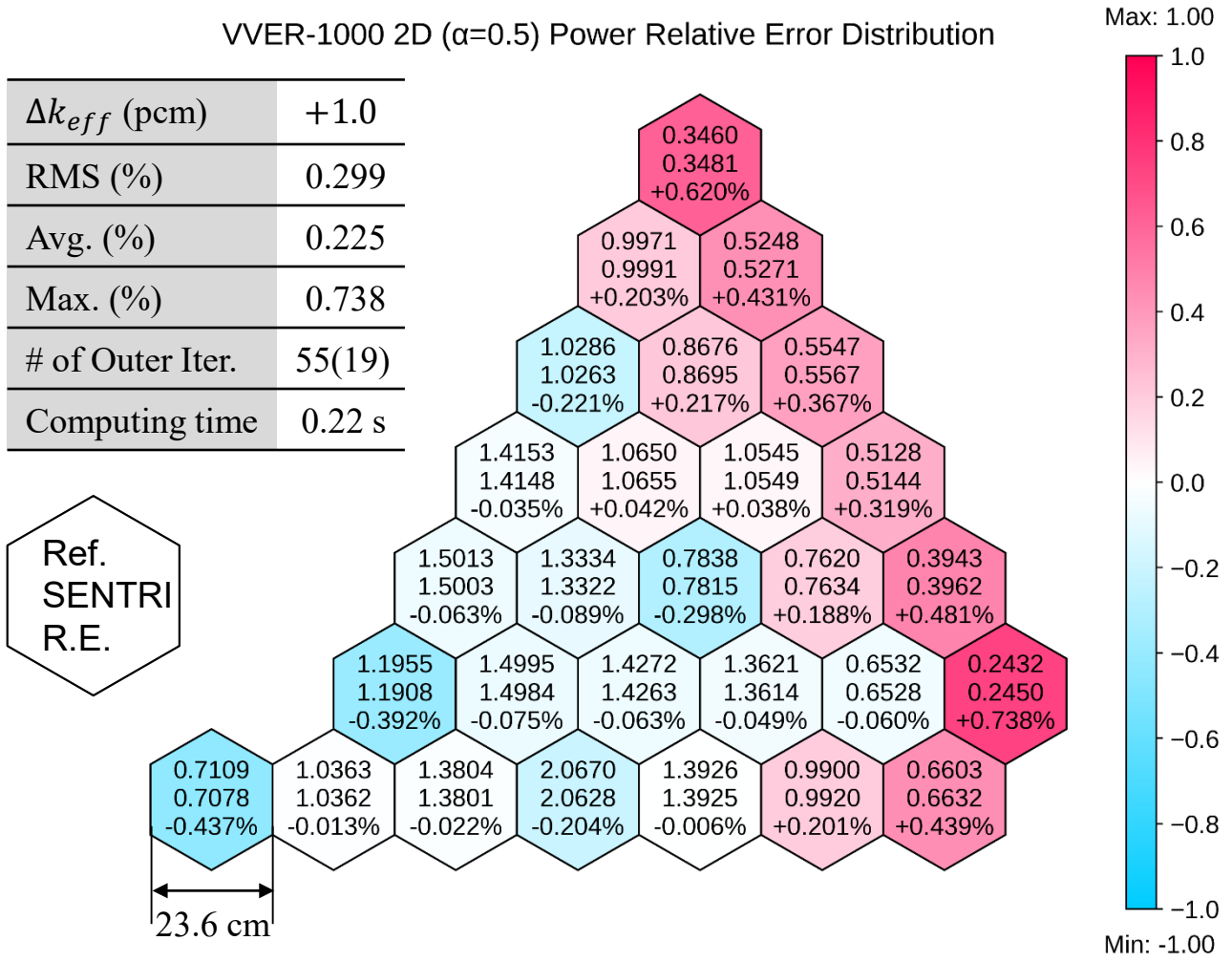
Δk_{eff} (pcm)	−13.0
RMS (%)	0.343
Avg. (%)	0.288
Max. (%)	0.675
# of Outer Iter.	37(15)
Computing time	0.15 s



3. Numerical Results

- **VVER-1000 2D 2G** ($\alpha = 0.500$)
  - $k_{eff} = 1.006495$ ($\Delta k_{eff} = +1.0\ pcm$)
  - RMS = 0.299 % | Avg. Abs. Rel. Err. = 0.225 % | Max. Abs. Rel. Err. = 0.738 %

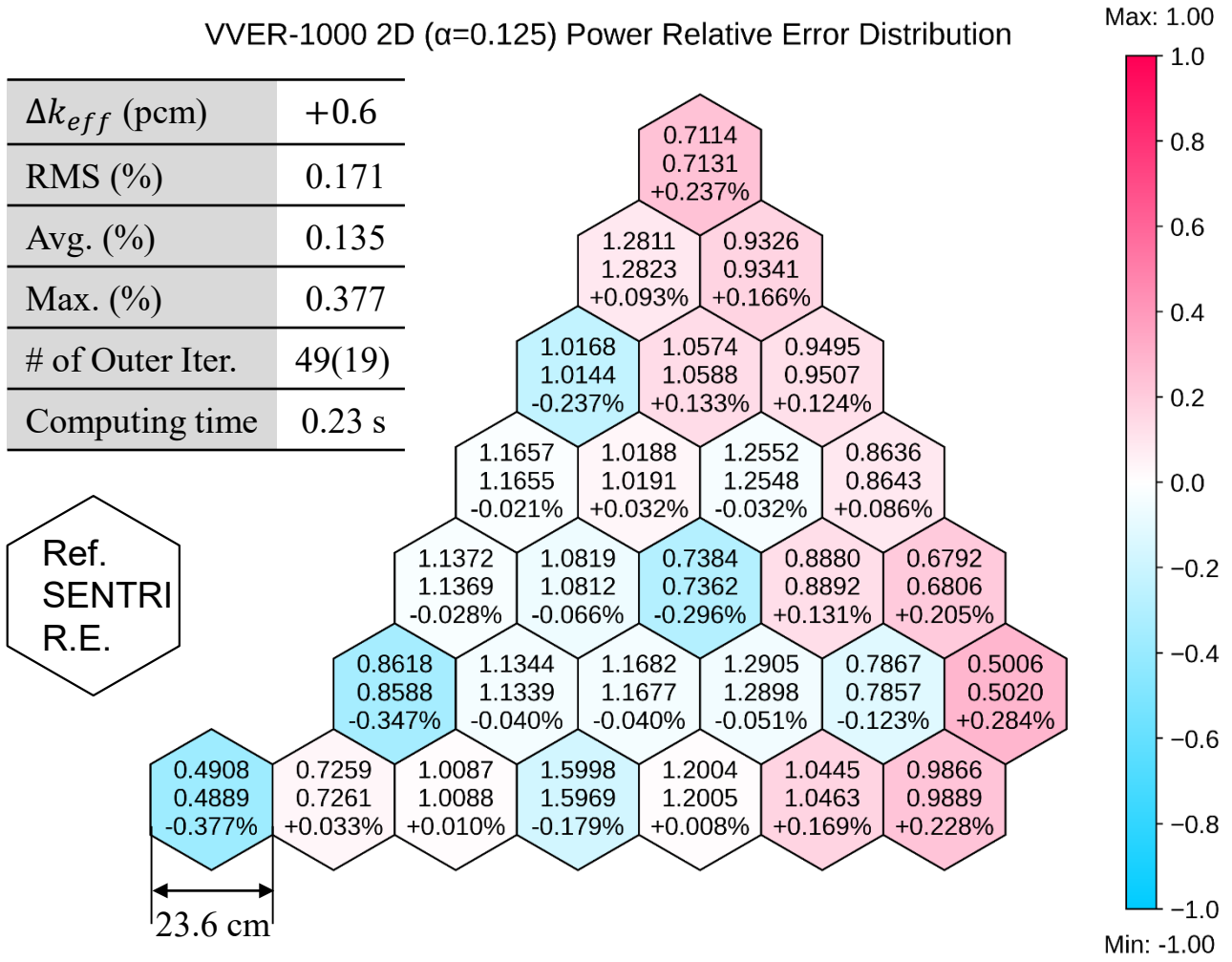
Δk_{eff} (pcm)	+1.0
RMS (%)	0.299
Avg. (%)	0.225
Max. (%)	0.738
# of Outer Iter.	55(19)
Computing time	0.22 s



3. Numerical Results

- **VVER-1000 2D 2G** ($\alpha = 0.125$)
  - $k_{eff} = 1.014413$ ($\Delta k_{eff} = +0.6\,pcm$)
  - RMS = 0.171 % | Avg. Abs. Rel. Err. = 0.135 % | Max. Abs. Rel. Err. = 0.377 %

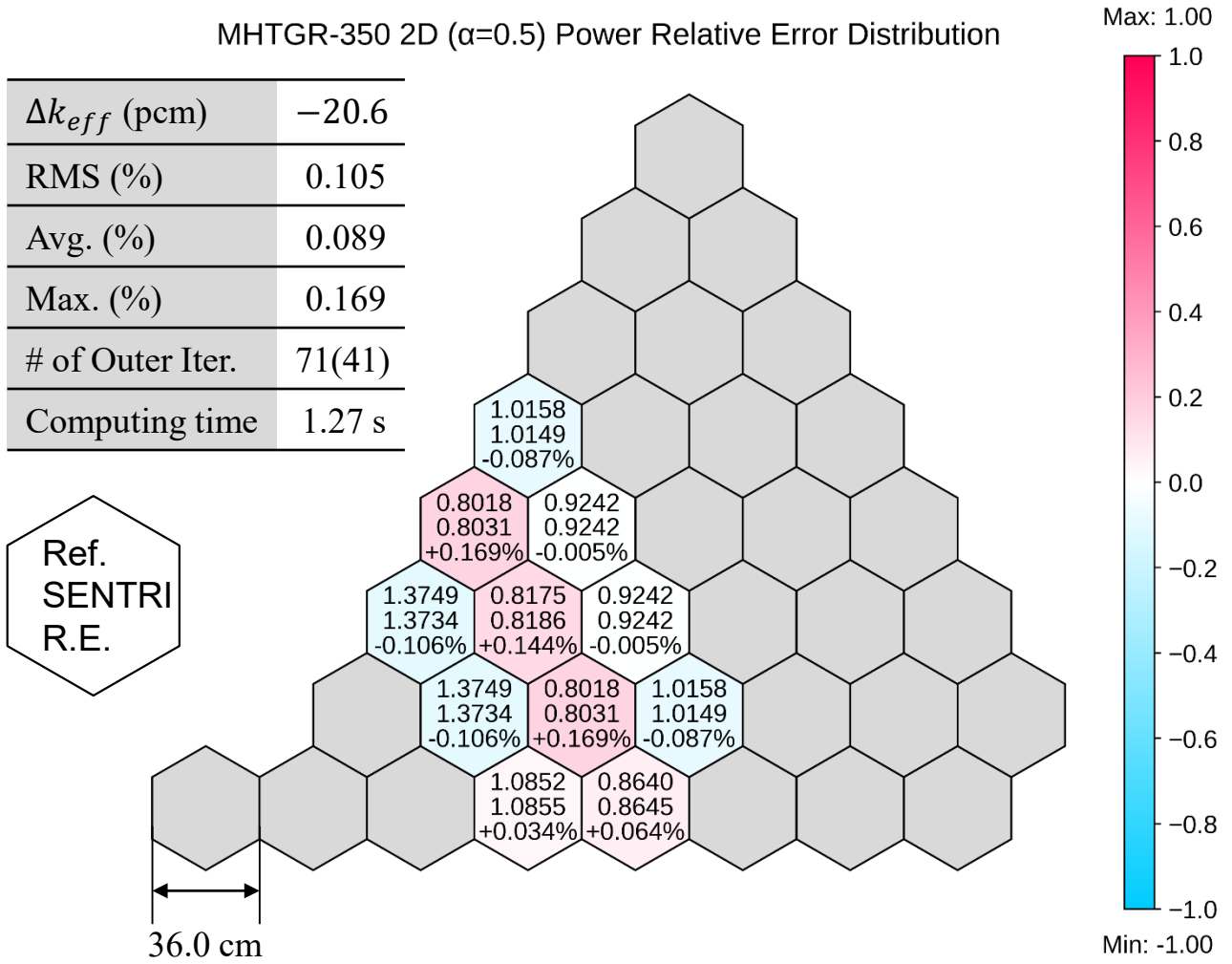
Δk_{eff} (pcm)	+0.6
RMS (%)	0.171
Avg. (%)	0.135
Max. (%)	0.377
# of Outer Iter.	49(19)
Computing time	0.23 s



3. Numerical Results

- **MHTGR-350 2D 10G** ($\alpha = 0.500$)
  - $k_{eff} = 1.093264$ ($\Delta k_{eff} = -20.6\,pcm$)
  - RMS = 0.105 % | Avg. Abs. Rel. Err. = 0.089 % | Max. Abs. Rel. Err. = 0.169 %

Δk_{eff} (pcm)	−20.6
RMS (%)	0.105
Avg. (%)	0.089
Max. (%)	0.169
# of Outer Iter.	71(41)
Computing time	1.27 s



3. Numerical Results

❑ Summary

Table II. Numerical results of the benchmark problems

Problem	Solver	Δk_{eff} (pcm)	Max Abs. Err.(%)	Avg. Rel. Err.(%)
VVER-440 2G ($\alpha = 0.5$)	TRIPEN	3	0.39	0.16
	TPEN	0	0.34	0.14
	HOPEN	13	0.61	0.29
	ANC-H	29	1.20	-
	AFEN[9]	23	1.25	0.52
	EFEN	-47	1.92	-
	A-SANM*	33	-	-
	SENTRI	-13	0.68	0.29
VVER-1000 2G ($\alpha = 0.5$)	TRIPEN	-7	0.26	0.12
	TPEN	-15	0.99	0.28
	HOPEN	30	3.84	1.52
	ANC-H	4	1.20	-
	AFEN[9]	32	3.73	1.52
	ABFEM-T	1	0.49	0.15
	A-SANM*	28	-	-
	SENTRI	1	0.74	0.23
VVER-1000 2G ($\alpha = 0.125$)	TRIPEN	-19	1.20	0.30
	TPEN	-15	0.90	0.20
	HOPEN	22	1.25	0.66
	ANC-H	9	0.50	-
	AFEN[9]	22	1.20	0.60
	ABFEM-T	-2	0.31	0.13
	SENTRI	1	0.38	0.14
MHTGR-350** 10G ($\alpha = 0.5$) [16]	AFEN[16]	-24	-	-
	SENTRI	-21	0.17	0.09

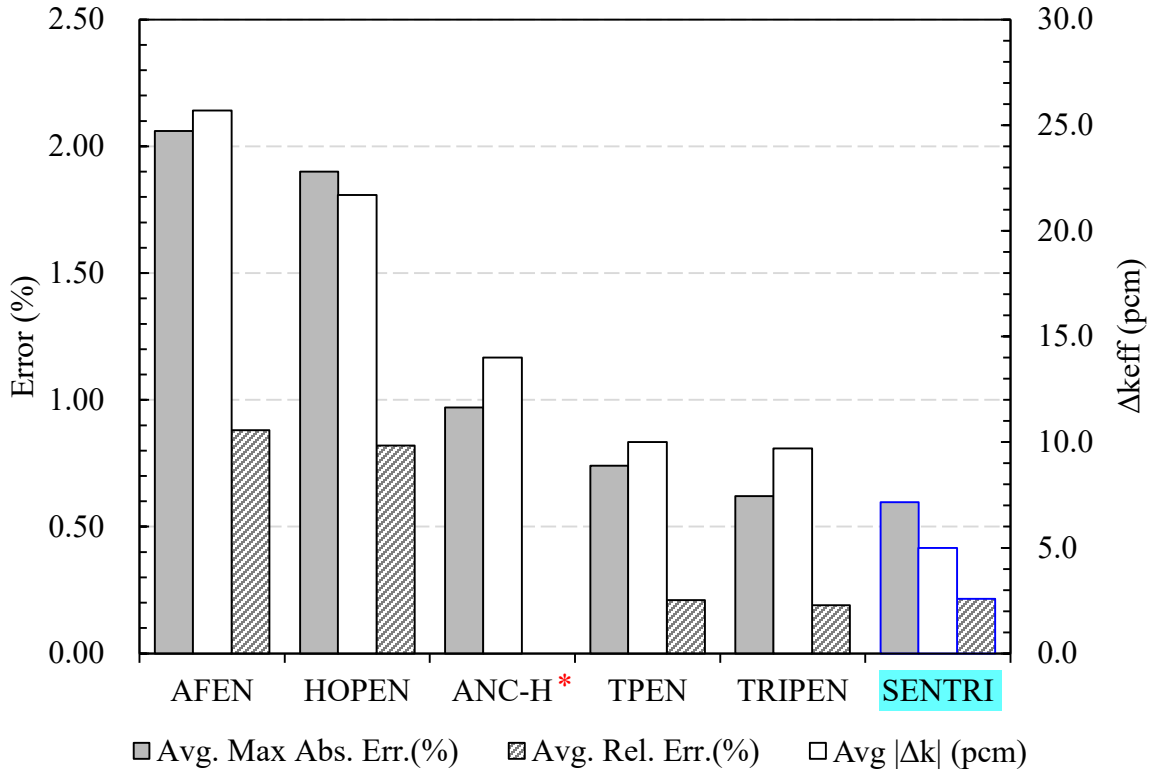
* Δk_{eff} from reported k_{eff} ; power errors reported only against McCARD[10]
** Obtained by Richardson extrapolation of FVM solutions with 1,536 and 6,144 triangles / hexagon.

3. Numerical Results

❑ Summary

- The average errors were evaluated for the solvers that provide results for all three benchmark problems
- Solvers: AFEN, HOPEN, ANC-H, TPEN, TRIPEN, SENTRI
- Benchmarks: VVER-440($\alpha = 0.5$), VVER-1000($\alpha = 0.5, 0.125$)

Comparison of average errors over the three benchmark problems



* The average relative power error of ANC-H is not available in the original reference [7][9]

Contents

1. **Introduction**
   - Motivation & Objectives
   - SENTRI

2. **Methodology**
   - Node definition & governing equation
   - Edge-segmented partial current
   - Basis functions
   - Source expansion
   - Solution Algorithm

3. **Numerical Results**
   - VVER440
   - VVER1000
   - MHTGR-350

4. **Conclusions & Future Works**

5. **References**

4. Conclusions & Future Works

❑ Successful introduction of half-edge segmented partial currents

- SENTRI was formulated without corner-point flux unknowns and tested on the VVER and MHTGR-350 diffusion benchmarks
- The absolute Δk_{eff} were within 13 pcm for VVER-440, 1 pcm for VVER-1000, and 21 pcm for the 10-group MHTGR-350 case.

❑ Comparison with a flat-source segmented-current method

- In VVER−440, SENTRI outperformed EFEN, which also uses segmented currents but a flat source, at a comparable mesh: **13** vs. 47 pcm and **0.68** vs. 1.92 %.
- EFEN needed about twice as many nodes to reach 22 pcm and 0.82 %, pointing to the flat source as the limiting factor.

❑ SANM accuracy without the corner-point flux

- SENTRI provides an alternative semi-analytic formulation using half-edge partial currents as interface constraints.
- Comparisons with A-SANM results indicate competitive eigenvalue accuracy for the tested benchmark

❑ Future Works

- Extension to three-dimensional core calculations
- Assessment of DF applicability and accuracy in heterogeneous problems

5. References

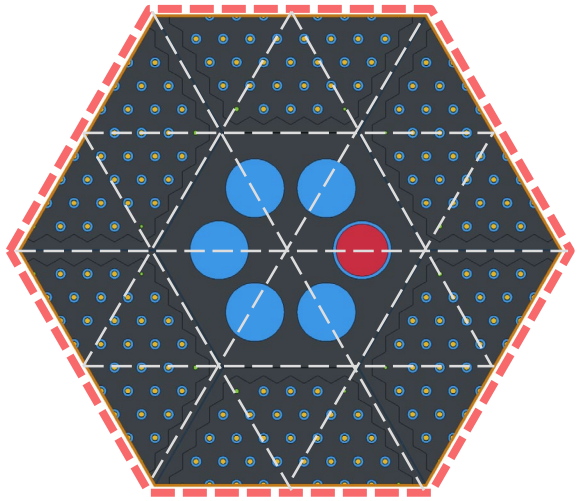
1. Black, G., Shropshire, D., Araújo, R., van Heek, A., 2023. "Prospects for nuclear microreactors: A review of the technology, economics, and regulatory considerations." *Nuclear Technology* **209**(sup1), S1–S20.
2. Cho, J.Y., Kim, C.H., 1998. "Higher order polynomial expansion nodal method for hexagonal core neutronics analysis." *Annals of Nuclear Energy* **25**(13), 1021–1031.
3. Noh, J.M., Cho, N.Z., 1994. "A new approach of analytic basis function expansion to neutron diffusion nodal calculation." *Nuclear Science and Engineering* **116**(3), 165–180.
4. Cho, N.Z., Noh, J.M., 1995. "Analytic function expansion nodal method for hexagonal geometry." *Nuclear Science and Engineering* **121**(2), 245–253.
5. Woo, S.W., Cho, N.Z., Noh, J.M., 2001. "The analytic function expansion nodal method refined with transverse gradient basis functions and interface flux moments." *Nuclear Science and Engineering* **139**(2), 156–173.
6. Chao, Y.A., Tsoulfanidis, N., 1995. "Conformal mapping and hexagonal nodal methods—I: Mathematical foundation." *Nuclear Science and Engineering* **121**(2), 202–209.
7. Chao, Y.A., Shatilla, Y.A., 1995. "Conformal mapping and hexagonal nodal methods—II: Implementation in the ANC-H code." *Nuclear Science and Engineering* **121**(2), 210–225.
8. Cho, J.Y., Joo, H.G., Cho, B.O., Zee, S.Q., 2001. "Hexagonal CMFD formulation employing triangle-based polynomial expansion nodal kernel." *Proc. M&C 2001*, Salt Lake City, UT, USA.
9. Kochunas, B., Seker, V., Ward, A., 2024. "Triangular polynomial expansion nodal method in AGREE." *Annals of Nuclear Energy* **206**, 110632.
10. Jang, J., Lee, D., 2024. "Development and verification of multigroup advanced semi analytic nodal method solver for HTGR analysis with MHTGR-350." *Annals of Nuclear Energy* **209**, 110818.
11. Wang, K., Wu, H., Cao, L., Wang, C., 2010. "Analytic basis function expansion nodal method for neutron diffusion equations in triangular geometry." *Proc. ICONE18*, Xi'an, China.
12. Li, Y., Wu, H., Cao, L., 2013. "Unstructured triangular nodal-SP3 method based on an exponential function expansion." *Nuclear Science and Engineering* **174**(2), 163–171.
13. Smith, K.S., 1986. "Assembly homogenization techniques for light water reactor analysis." *Progress in Nuclear Energy* **17**(3), 303–335.
14. Kim, D.S., Cho, N.Z., 2003. "The analytic function expansion nodal (AFEN) method with half-interface averaged fluxes in mixed geometry nodes for analysis of pebble bed modular reactor (PBMR) cores." *Journal of Nuclear Science and Technology* **40**(5), 291–297.
15. Cho, J.Y., Lee, H.C., Song, J.S., 2015. “DeCART equivalent group constants generation for hexagonal TPEN method.” *Proc. RPHA15*, Jeju, Korea.
16. Noh, J.M., 2020. “A response matrix method for the refined analytic function expansion nodal (AFEN) method in the two-dimensional hexagonal geometry and its numerical performance.” *Nuclear Engineering and Technology* **52**, 2422–2430.
17. Downar, T., Xu, Y., Seker, V., Hudson, N., 2009. “Theory manual for the PARCS kinetics core simulator module.” University of Michigan, Ann Arbor, MI, USA.

Thank you!

Back-up Slide

❑ DF Application in SENTRI

- Toy problem: One control rod(B_4C) insertion in a graphite block surrounded by fuel blocks(UO_2)
- Reflective boundary condition, Block pitch = 36.1 cm, CR diameter = 8 cm
- One DF per edge: 3 DFs per triangular node per group



<Fig. A1. Problem configuration>

Table A1. Reference reproduction with DFs

# of Group	Case	k_{eff}	Δk_{eff}	Power RMS
2	Serpent (MC)*	0.878235±9.7 pcm	-	-
	SENTRI w/o DF	0.871483	-675.1 pcm	4.01 %
	SENTRI w/ DF	0.878283	+4.8 pcm	0.02 %
5	Serpent (MC)**	0.878286±5.9 pcm	-	-
	SENTRI w/o DF	0.869978	-830.8 pcm	4.02 %
	SENTRI w/ DF	0.878286	0.0 pcm	0.02 %

* 2G: 300k histories / cycle, 75 inactive , 300 active cycles
** 5G: 750k histories / cycle, 75 inactive , 300 active cycles